Insight into β-hairpin stability: a structural and thermodynamic study of diastereomeric β-hairpin mimetics†

Máté Erdélyi,[a,b] Vratislav Langer,[c] Anders Karlén[b] and Adolf Gogoll*[a]

[a] *Department of Organic Chemistry, Uppsala University, Box 531, 751 21 Uppsala, Sweden. E-mail: adolf@kemi.uu.se; Fax: +46 18 512 524*

[b] *Department of Medicinal Chemistry, Uppsala University, Box 574, 751 23 Uppsala, Sweden. Fax: +46 18 471 4474*

[c] *Department of Environmental Inorganic Chemistry, Chalmers University of Technology, 412 96 Göteborg, Sweden. Fax: +46 31 772 2853*

Received (in London, UK) 10th December 2001, Accepted 23rd April 2002
First published as an Advance Article on the web 6th June 2002

Two diastereomers of a model β-hairpin peptide mimetic were synthesized and studied with a combination of experimental (NMR, X-ray, CD, MS, IR) and computational methods (Monte Carlo/molecular mechanics calculations). The secondary structure-stabilizing effects of hydrophobic interactions and hydrogen bonding were investigated. Comparison of the extent of folded hairpin population in non-competitive, polar aprotic, and polar protic solvents illustrates the critical role of intramolecular hydrogen bonding on hairpin stability. Investigation of ^{1}H NMR melting curves of the diastereomeric compounds in a variety of solvents allowed an evaluation of the role of hydrophobic effects on secondary structure stabilization to be made.

Introduction

β-Hairpins have been shown to play a key role in vital as well as in pathological processes. They frequently participate in protein–protein,[1] protein–RNA,[2] and protein–DNA[3] recognition. Prion diseases,[4] Alzheimer's disease,[5] the IgE-mediated allergic response,[6] the interaction of bacterial cell surface-associated protein with IgG,[7] and HIV gp120 binding to human T-cell surface protein CD4[8] are some examples involving the β-hairpin secondary structure element in biological processes. In spite of its significance, the principles underlying hairpin stability are still unresolved, perhaps because of the general difficulty of investigating hairpins, due to their low solubility and high propensity to aggregate.[9,10] Despite these obstacles, several examples of naturally occuring β-hairpins[11] and hairpin mimetics[12] have been reported recently.

While it is known that several factors affect hairpin stability,‡ their relative importance is not well understood. A general difficulty when trying to evaluate the impact of one particular stabilizing factor is the presence of several, possibly cooperative, weak interactions.[23c,26] A deeper understanding of the influence of different types of non-covalent interactions on conformational equilibria is desirable for both theoretical and practical reasons. For a quantitative evaluation of such interactions, we have investigated two diastereomers of a model hairpin mimetic (Fig. 1). The similarity of these two diastereomers made it possible to separately study the role of hydrophobic interactions, since the effects of the turn region, solvent, hydrogen bonding, electrostatic effects, and chain length are identical. Such a selective examination of one non-covalent, weak interaction in the presence of other cooperative factors has not been attempted previously and is, therefore, of general interest.

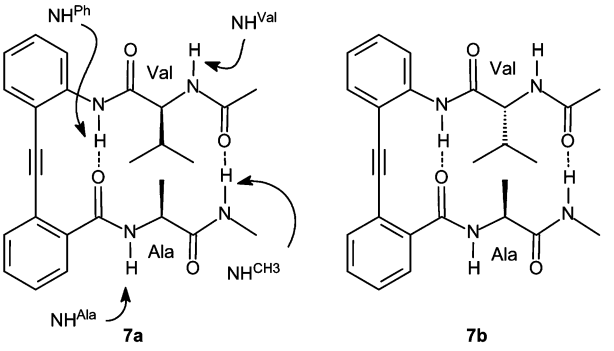

Fig. 1 The investigated model β-hairpin mimetics.

Gellman and co-workers have shown that the configuration of the amino acids in the turn region affects hairpin stability.[16c,d] However, many of the turn mimics reported are achiral and, therefore, have no preferred twist.[4b,9a,12,16e–i,23a,b,27b] To avoid complications possibly arising from the turn region, the known rigid, achiral tolan turn mimic[16e,f] was chosen for this investigation, focusing on the effect of non-covalent side-chain interactions on hairpin conformational stability. For our model study, we selected the shortest possible amino acid strands which allow the formation of two intramolecular hydrogen bonds. By selecting small, nonpolar, nonaromatic amino acid side chains, we could simultaneously minimize the size of the model system as well as the interactions between the turn mimetic and the peptide strands. To date, this is the

† Electronic supplementary information (ESI) available: temperature and concentration-dependent chemical shifts and melting curves of the investigated molecules in different solvents and details of the X-ray analysis. See http://www.rsc.org/suppdata/nj/b1/b111241d/

‡ For example, the β-sheet-forming tendencies of amino acids,[8b,13,14] the length of the peptide strands,[15,16] the type of β-turn[8b,9c,11b,13c,17] or the characteristics of the β-turn mimetic,[12b,16c,d] the side-chain properties,[8b,18] context effects,[8b,13a,19] steric factors,[20] the role of interchain hydrogen bonds,[16c,21,22] β-branching in amino acid side chains, hydrophobic cluster formation,[8b,13,23,24] and electrostatic interactions.[9c,25]

 DOI: 10.1039/b111241d

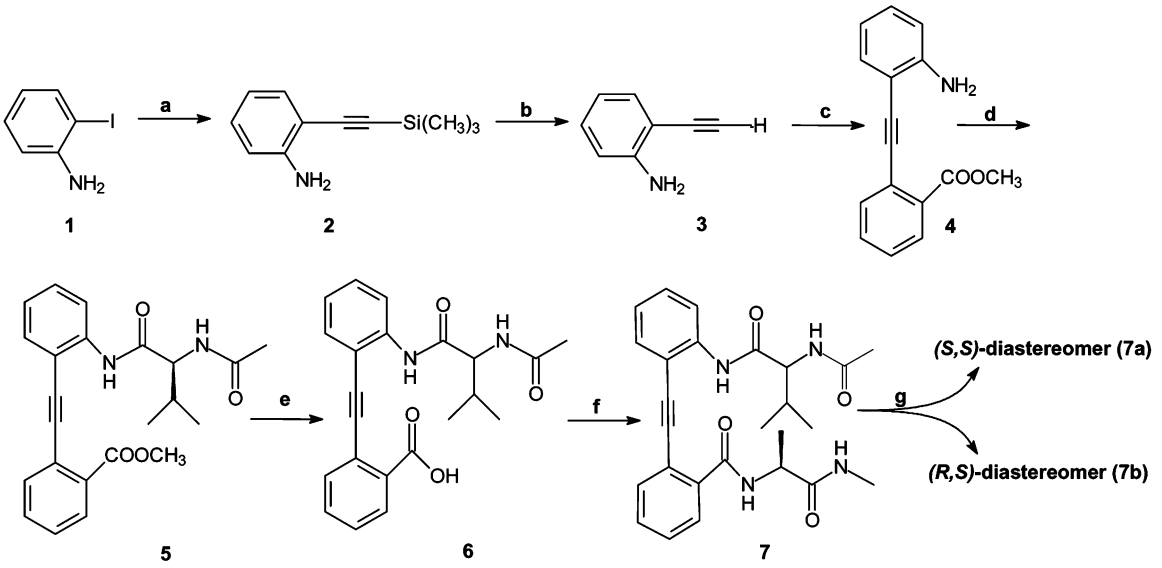

Scheme 1 Outline of the synthesis of the diastereomeric hairpin mimetics. *Reagents and conditions*: (a) $Me_3SiC{\equiv}CH$, $Pd(PPh_3)_2Cl_2$, CuI, Et_2NH, 120 °C, 5 min, 98%; (b) $KF{\cdot}2H_2O$, MeOH, r.t., 7 h, 97%; (c) methyl-2-iodobenzoate, $Pd(PPh_3)_2Cl_2$, CuI, Et_2NH, 120 °C, 5 min, 78%; (d) BSA, HATU, $^{i}Pr_2NEt$, (*S*)-2-acetylamino-3-methylbutyric acid, r.t., 72 h, 52%; (e) $KO^{t}Bu$, Et_2O, 10 h, 99%; (f) HATU, $^{i}Pr_2NEt$, (*S*)-2-amino-*N*-methyl-propionamide, r.t., 1 h, 51%; (g) HPLC: 55% **7a**, 45% **7b**.

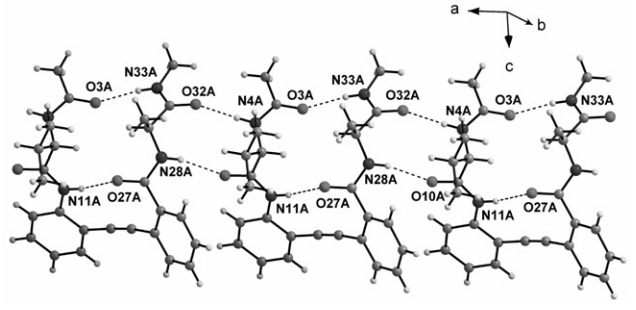

Fig. 2 Hydrogen bonds connecting molecules of **7a** in an infinite ribbon in the *a* direction. Hydrogen bonds, intramolecular: H(11a)–O(27a) = 2.33, H(33a)–O(3a) = 2.03 Å; intermolecular: H(4a)–O(32a) = 2.07, H(28a)–O(10a) = 2.16 Å.

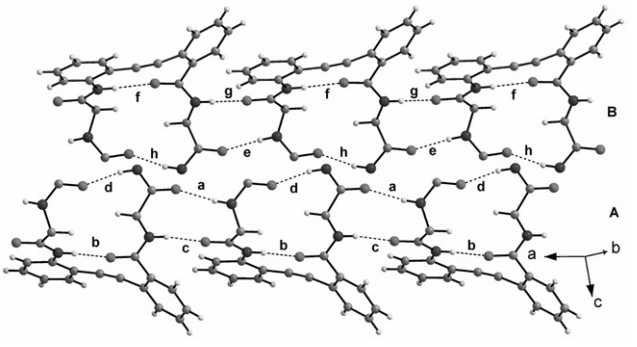

Fig. 3 Hydrogen bonds connecting conformers A and B of **7a** in two separate ribbons parallel to the *a* direction. Hydrogen bonds in A, see Fig. 2. Hydrogen bonds in B, intramolecular: H(11b)–O(27b) = 2.43, H(33b)–O(3b) = 1.95 Å; intermolecular: H(4b)–O(32b) = 2.01, H(28b)–O(10b) = 2.17 Å. End methyl groups and Val side-chain atoms were omitted for clarity. Symbols refer to those in Table S7 (ESI).

first investigation of hairpins which differ in the configuration of one of the peptide strands.

Results and discussion

Synthesis

Scheme 1 outlines the methodology used to prepare the (*S*)-Val, (*S*)-Ala (**7a**) and (*R*)-Val, (*S*)-Ala (**7b**) derivatives of 2-amido-2′-carboxamidotolane (**7**).

X-Ray analysis

The crystallographic analysis of diastereomer **7a** (Fig. 2 and 3) shows that the molecule has a high tendency to form 10 and 14-membered ring C=O···H–N hydrogen bonds, as are commonly observed in β-hairpins. The asymmetric unit of the triclinic crystal system contains two independent molecules, showing a slight difference in hydrogen bond lengths. These two conformers of **7a** give rise to two distinct ribbon structures (see ESI). No crystals suitable for X-ray analysis could be obtained for **7b**.

Conformational analysis by molecular mechanics calculations

Monte Carlo simulation combined with molecular mechanics energy minimization in the OPLS-AA force field was used to predict the conformation population for the two diastereomers in chloroform solution. Conformations within 25 $kJmol^{-1}$ of the lowest energy minimum were examined. The obtained structures were then classified as "hairpin" or "non-hairpin", depending on the presence of two interchain hydrogen bonds. The conformations identified as β-hairpin amounted to a population of 15.6 and 20.7% at 298 K for diastereomers **7a** and **7b**, respectively, using the Boltzman equation for the calculation.

Conformational analysis in solution

Where solubility in water was an issue, similarly to other β-hairpin studies,[9b,16,18,22] the investigations were made in methanol, dimethylsulfoxide, and chloroform solutions.

Circular dichroism

The CD spectrum of diastereomer **7a** recorded in methanol shows the characteristic perturbation feature for tolan

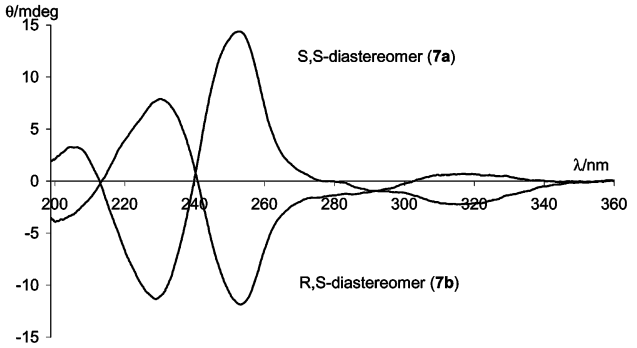

Fig. 4 The CD spectra of the hairpin diastereomers (methanol solution).

derivatives,[16e,f] as well as a positive band at 209 nm and an intense negative band at 228 nm, typical of a β-turn[28] (Fig. 4). We presume that the small size of the mimetic is responsible for its CD spectrum resembling more that of β-turns than that of β-hairpins.§ In general, the CD spectra of β-structures tend to depend on the length of the side chains and the twist of the turn region.[30] The reversed chirality at one centre in diastereomer **7b** gave rise to a spectrum in methanol that resembled, apart from the intensities, the mirror image of the spectrum of **7a**. This feature is unusual for diastereomer pairs and it suggests that the contributions of the chromophores near to the valine alpha carbon are dominant over the contribution of the chromophores near to the alanine alpha carbon. The observed CD spectra allow the configurational assignment of the two diastereomers, with the diastereomer **7a** showing a spectrum characteristic for β-structures consisting of natural amino acids. This assignment of the absolute configuration at C_α of valine was confirmed by X-ray and 1D NOE NMR experiments. Finally, the different magnitudes of the ellipticities at 228 nm might suggest that the diastereomer **7a** has a slightly higher population of β-structure conformation than **7b**.

IR spectra

The presence of intramolecular amide–amide hydrogen bonding as an indicator of hairpin folding was probed by analysing the amide N–H stretch region in chloroform solution. In this spectral region, both the **7a** and **7b** diastereomers exhibited an intense IR band at 3307–3308 cm^{-1} (hydrogen-bonded N–H vibration) and a less intense band at 3413 cm^{-1} (non-hydrogen-bonded N–H vibration).[16d,27,29] These results indicate that both hydrogen-bonded and non-bonded amide protons were present in the solutions of both diastereomers, with no signs of any differences.

Mass spectra

The two diastereomers show an unexpected difference in their ESI mass spectra (Fig. 5). Whereas the spectrum of **7a** contains only the $[M+H]^+$ and $[M+Na]^+$ ions, the spectrum of **7b** shows, in addition to $[M+1]^+$ and $[M+Na]^+$, several other fragment ions, of which $m/z = 322$ is the base peak. Such different behavior of diastereomers in mass spectra has been reported before only in a very few cases.[31] The differences in the population equilibria of the possible conformations—showing various extents of accessibility for ionization—is presumed to be responsible for the differences in the spectra of the diastereomers. This assumption is supported by the results from FD and FAB MS investigations of diastereomeric tripeptide ester derivatives.[32]

§ Usually, the hairpin conformation in peptides containing natural L-amino acids is indicated by a strong negative CD band at *ca.* 216–222 nm.[16a,29]

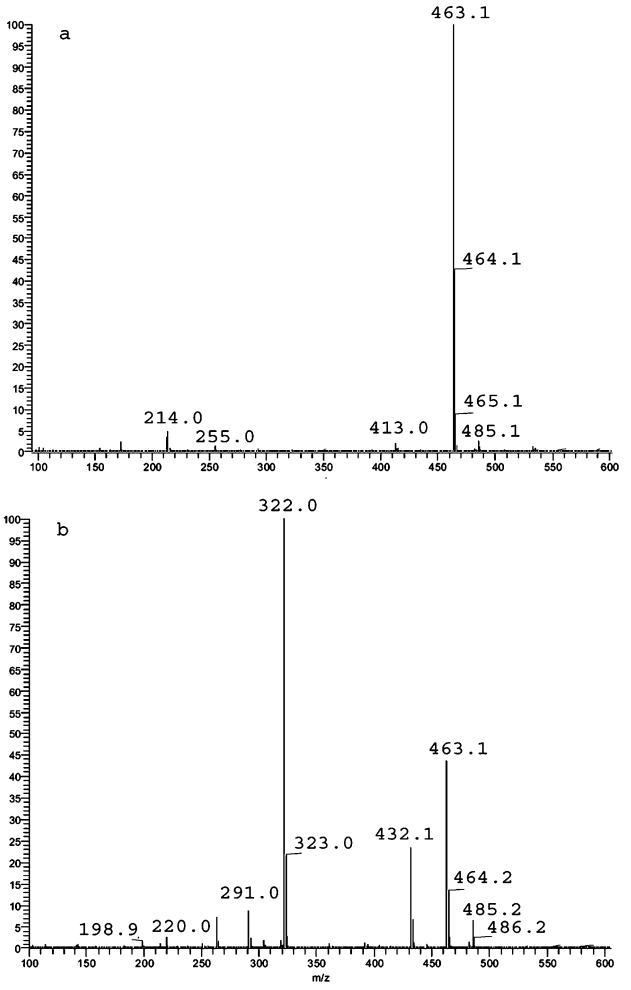

Fig. 5 ESI mass spectra of (a) **7a** and (b) **7b**.

NMR investigation

Structural assignment. The ^1H and ^{13}C NMR spectra of **7a** and **7b** have been fully assigned in several solvents using data from COSY,[33] HSQC,[34] COLOC,[35] NOESY,[36] ROESY,[37] and gHMBC[38] experiments. The ^1H chemical shift assignments are presented in Table 1. The absolute configuration of the two hairpin diastereomers **7a** and **7b** was confirmed using 1D NOE difference[39] spectra (Fig. 6). These spectra were run on $CDCl_3$ solutions at room temperature after exchange of all amide NH protons with deuterium. As expected, interstrand NOEs were observed between the methyl groups of valine and alanine for the **7a** diastereomer, but not the **7b** diastereomer (Fig. 1). Similar effects were obtained by irradiation of either one of the valine and alanine methyl groups. Interestingly, these small effects could not be observed without deuterium exchange. This further confirms the configurational assignment made by CD spectroscopy and X-ray crystallography.

Absence of aggregation behavior. Concentration dependency of amide chemical shifts. The absence of intermolecular interactions in solution was probed by investigating the concentration dependency of $\Delta\delta_{NH}$ for all amide protons. The variation of $\Delta\delta_{NH}$ as a function of concentration in chloroform, methanol and DMSO solution was negligible (see ESI).

Table 1 ^{1}H chemical shift assignments (δ) for the side chains of β-hairpin mimetics **7a** and **7b** at 298 K in DMSO-d_6, CH_3OH–CD_3OD (2:1), and $CDCl_3$ solution

	7a			**7b**		
Residue	DMSO-d_6	CH_3OH–CD_3OD	$CDCl_3$	DMSO-d_6	CH_3OH–CD_3OD	$CDCl_3$
NH^{Ph}	9.47	9.54	9.34	9.38	9.54	9.68
NH^{CH_3}	7.91	8.02	7.89	7.77	8.02	7.87
NH^{Ala}	8.77	8.54	7.08	8.72	8.54	6.96
NH^{Val}	8.21	8.21	6.54	8.17	8.21	6.64
Ala-CH_α	4.58	4.68	5.32	4.63	4.68	5.26
Ala-CH_3	1.30	1.41	1.48	1.29	1.41	1.36
CH_3^{NHAla}	2.51	2.54	2.76	2.57	2.55	2.81
Val-CH_α	4.88	5.04	5.50	4.82	5.04	5.64
Val-CH_β	2.11	2.20	2.33	2.12	2.20	2.25
Val-$CH_{\gamma1}$	0.90	0.96	1.05	0.89	0.96	0.93
Val-$CH_{\gamma2}$	0.88	0.95	0.95	0.88	0.95	0.87
CH_3^{COVal}	1.92	1.99	2.08	1.89	1.99	2.11

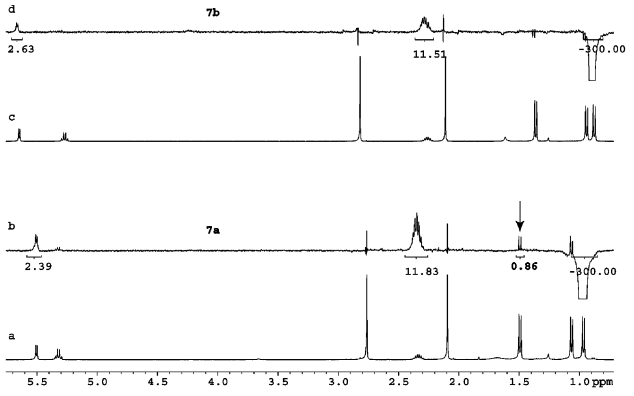

Fig. 6 Aliphatic region of the 1D NOE difference spectra for the diastereomers **7a** and **7b**, (400 MHz, 25 °C, $CDCl_3$ solution). (a) **7a**, reference spectrum; (b) **7a**, NOE difference spectrum, one Val-Me irradiated; (c) **7b**, reference spectrum; (d) **7b**, NOE difference spectrum, one Val-Me irradiated. Integrated steady state NOEs are shown below the signals (in %, normalized to the irradiated methyl group = −300%).

Evidence for hairpin conformation in solution interstrand NOEs. In $CDCl_3$, β-hairpin formation is indicated by the observation of interstrand NOEs. The strongest NOEs were observed between the alpha protons of valine and alanine (Fig. 7). The NOEs between the signals of these protons were much weaker in DMSO-d_6 solution for both diastereomers, indicating that the β-hairpin conformations are more populated in the non-competitive solvent $CDCl_3$. These NOEs could not be studied in methanol solution due to signal overlap.

Solvent effects on amide chemical shifts. In agreement with the low energy conformation obtained by computation and X-ray studies, the NH^{Ph} and NH^{CH_3} protons (see Fig. 1 for assignment) for both diastereomers were much less affected by changes in the solvent than were the signals due to the NH^{Ala} and NH^{Val} protons (Table 1). For diastereomer **7a**, upon changing the solvent from $CDCl_3$ to DMSO-d_6, the chemical shifts of the NH^{Ph} and the NH^{CH_3} signals changed by $\Delta\delta_{solv} = 0.1$ and 0.01 ppm, respectively, whereas the chemical shifts of NH^{Ala} and NH^{Val} changed by $\Delta\delta_{solv} = 1.6$ ppm ($\Delta\delta_{solv} = \delta_{DMSO} - \delta_{CDCl_3}$). The same trends were observed when changing the solvent from $CDCl_3$ to methanol [$\Delta\delta_{solv} = 0.2$ (NH^{Ph}), −0.1 (NH^{CH_3}), 1.4 (NH^{Ala}) and 1.6 ppm (NH^{Val})]. For the diastereomer **7b**, the amide protons showed similar behavior. Thus, changing the solvent from $CDCl_3$ to DMSO-d_6 resulted in chemical shift changes for the NH^{Ph} and the NH^{CH_3} proton resonances of $\Delta\delta_{solv} = -0.3$ −0.3 and −0.1 ppm, respectively, while the NH^{Ala} and NH^{Val} protons showed $\Delta\delta_{solv} = 1.8$ and 1.6 ppm, respectively. When changing the solvent from $CDCl_3$ to methanol, the shift changes for NH^{Ph} and NH^{CH_3} were $\Delta\delta_{solv} = -0.3$ and 0.1 ppm, while for both the NH^{Ala} and the NH^{Val} protons, $\Delta\delta_{solv} = 1.6$ ppm. This observation supports a β-hairpin conformation, in which the NH^{Ph} and NH^{CH_3} protons are hydrogen bonded, and NH^{Ala} and NH^{Val} are not (Fig. 1).[28]

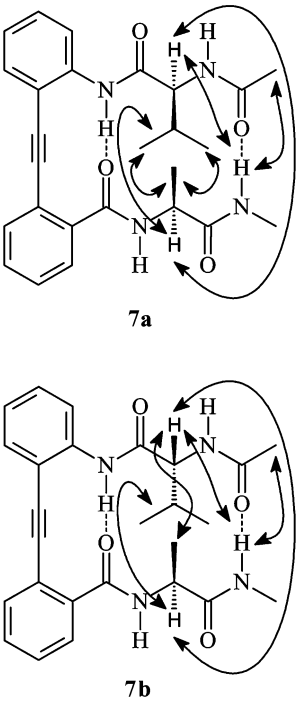

Fig. 7 Interstrand NOEs observed in $CDCl_3$ solution (400 MHz, 25 °C).

Amide proton temperature coefficients ($\Delta\delta/\Delta T$). A comparison of the temperature coefficients for the amide protons (Table 2) provided further evidence for folded β-hairpin conformations in which protons NH^{Ph} and NH^{CH_3} are intramolecularly hydrogen bonded.¶

¶ Temperature coefficients, $(\delta_{T_{high}} - \delta_{T_{low}})/(T_{high} - T_{low})$, are obtained as negative numbers, but are reported as positive values, in accordance with the accepted literature procedure: H. Kessler, *Angew. Chem.*, 1982, **94**, 509.

Table 2 Amide temperature coefficients[a] in DMSO-d_6, CH_3OH–CD_3OD (2:1), and $CDCl_3$ solution

	7a			7b		
Residue	DMSO-d_6	CH_3OH–CD_3OD	$CDCl_3$	DMSO-d_6	CH_3OH–CD_3OD	$CDCl_3$
NH^{Ph}	3.1	2.6	0.4	2.6	2.5	0.7
NH^{CH_3}	4.5	4.8	4.2	3.6	4.8	4.1
NH^{Ala}	5.9	7.3	1.4	5.5	7.1	1.7
NH^{Val}	5.3	7.7	1.7	5.1	7.6	1.8

[a] The amide proton temperature coefficients, $\Delta\delta(NH)/\Delta T$ (in ppb K^{-1}) were measured for 8 mmol dm^{-3} samples in DMSO over the temperature range 298–418 K, in CH_3OH–CD_3OD (2:1) over the range 178–323 K, and in $CDCl_3$ over the temperature range 298–333 K.

Table 3 Thermodynamic parameters for unfolding of β-hairpin mimetic **7a** and **7b** in DMSO-d_6 and CH_3OH–CD_3OD (2:1) solutions

	Solvent	T_m/K	ΔH_m/kJ mol^{-1}	ΔS_m/J K^{-1} mol^{-1}	$\Delta G^\circ_{298\ K}$/kJ mol^{-1}
7b	DMSO-d_6	388 ± 5.8	16.5 ± 0.6	42.5 ± 0.9	3.8 ± 0.3
7a	CH_3OH–CD_3OD	306.9 ± 7.5	11.2 ± 0.6	36.4 ± 1.3	0.32 ± 0.3
7b	CH_3OH–CD_3OD	301.4 ± 3.8	11.1 ± 0.4	36.9 ± 1.9	0.12 ± 0.1

In the polar, aprotic dimethylsulfoxide-d_6, the amide protons NH^{Ala} and NH^{Val} have high temperature coefficients (> 5 ppb K^{-1}) in both diastereomers, showing that they are solvent exposed. The amide proton NH^{Ph} has the lowest temperature coefficient. The NH^{CH_3} protons in both diastereomers show an intermediate behavior, indicating that they are in equilibrium between hydrogen-bonded and non-hydrogen-bonded states.[28,29]

In polar, protic methanol, the temperature coefficients of the two diastereomers are very similar. The NH^{Ala} and NH^{Val} amide protons may be solvent accessible, while proton NH^{CH_3} is in equilibrium between hydrogen-bonded and non-hydrogen-bonded states. NH^{Ph} has a temperature coefficient of less than than 3 ppb K^{-1} and could, therefore, be hydrogen bonded.

In apolar, aprotic $CDCl_3$, the amide temperature coefficients are more difficult to interpret,[16a,27a] and can only be understood in combination with other parameters, such as chemical shift (Table 1) and its solvent-dependent behavior ($\Delta\delta_{solv}$, see preceding section). According to the classification introduced by Nowick and Soth.,[16a] the protons NH^{Ala} and NH^{Val} are not hydrogen bonded in any of the diastereomers (low δ, low $\Delta\delta/\Delta T$, high $\Delta\delta_{solv}$). Proton NH^{Ph} may be strongly hydrogen bonded in both mimetic **7a** and **7b** (high δ, low $\Delta\delta/\Delta T$, low $\Delta\delta_{solv}$). However, the NMR parameters of this proton should be interpreted carefully because the phenyl ring attached to NH^{Ph} affects its solvent accessibility and chemical shift. Proton NH^{CH_3} could be in equilibrium between hydrogen-bonded and non-hydrogen-bonded states (intermediate δ, high $\Delta\delta/\Delta T$, low $\Delta\delta_{solv}$). In $CDCl_3$ solution, below room temperature, both hairpin mimetics showed a tendency for self-association, indicated by the rapid change in the temperature coefficients of the NH^{Ala} and NH^{Val} protons.‖

Thermodynamic analyses

A common method for quantitative thermodynamic description of hairpin stability is investigation of the protein melting curve.[13b,25,26,40] We have therefore investigated the temperature dependency of chemical shifts of side-chain and alpha protons.[40a,b]

Results for DMSO-d_6 solution. The ^1H chemical shift measurements were made over the temperature range 298 to 418 K. Data for Ala-CH_3, Val-CH_3, Val-CH_β, Val-CH_α, and CH_3^{NHAla} were investigated.** The analysis of these melting curves lead to the conclusion that diastereomer **7b** has its melting point (T_m) at approximately 388 K (Table 3), while the melting point of diastereomer **7a** is likely to be higher than 418 K, the highest temperature accessible for our NMR equipment.†† By comparing the melting curves, we conclude that the β-hairpin conformation of mimetic **7a** is significantly more stable in the polar aprotic solvent DMSO than is that of its diastereomer **7b** ($\Delta T_m > 30$ K).

Results for methanol solution. The chemical shifts of Val-CH_3, CH_3^{COVal}, and CH_3^{NHAla} were measured over the temperature range 178 to 328 K.‡‡ The calculated thermodynamic parameters are reported in Table 3. They indicate that in the polar protic solvent methanol, the two diastereomers have similar stabilities within experimental error.

Results for $CDCl_3$ solution. The melting curve was measured over the temperature range 213 to 328 K. Analysis of the reciprocal temperature curve suggests that the inflexion point of the melting curve might be above the boiling point of $CDCl_3$ and, therefore, the thermodynamic constants can not be calculated. This observation leads to the assumption that in the apolar, aprotic solvent $CDCl_3$, both diastereomers are highly folded.

Entropic and enthalpic contributions to β-hairpin stability

Comparison of the thermodynamic parameters of one of the diastereomer hairpins in different solvents provides quantitative information on the importance of interstrand hydrogen bonding, and allows a comparison of the conformer-stabilizing

‖ For diastereomer **7a**, $\Delta\delta/\Delta T$ calculated between 213 and 273 K was 2.4 ppb K^{-1} for NH^{Ala} and 4.6 ppb K^{-1} for NH^{Val}. For the diastereomer **7b**, the corresponding values were 5.6 (NH^{Ala}) and 6.9 ppb K^{-1} (NH^{Val}). The corresponding values for solutions at or above room temperature were considerably lower (Table 2).

** Analyses of Ala-CH_α and CH_3^{COVal} were not performed because of the small difference in chemical shift for these protons between the folded and unfolded states ($|\delta_F - \delta_U| < 0.03$ ppm).[40a,b]

†† The fact that the inflexion point of the melting curve of **7a** could not be observed ruled out the possibility of calculating exact thermodynamic parameters for this diastereomer.

‡‡ The NMR signals of alpha protons were omitted from the calculations because of signal overlap. The change in chemical shift upon unfolding for Ala-CH_3 was less then 0.03 ppm and was, therefore, not investigated. The iterative curve fitting for the chemical shift of Val-CH_β did not converge. The first-order derivatives of the melting curves for both diastereomeric compounds is available in the ESI.

role of hydrophobic and hydrogen-bonding interactions to be made. The folding of the model compound **7b** in methanol solution is exothermic, and the enthalpic (ΔH) and entropic ($-T\Delta S$) contributions to its stability at room temperature are approximately equal (Table 3). When changing the solvent to DMSO, the folding still remains exothermic, but becomes enthalpy driven. The increasing role of enthalpy upon changing the solvent indicates the greater influence of interstrand hydrogen bonding on hairpin folding in the less polar aprotic medium, in which, as expected, hydrophobic stabilization is not as effective. The negative entropic contribution to folding suggests that the hydrophobic effect is not the dominating stability-determining factor in our model system. As the folding process becomes more exothermic (ΔH upon unfolding is more positive in DMSO than in methanol, *i.e.* ΔH upon folding is more negative), the entropy term gets increasingly more negative. Thus, the stronger hydrogen-bonding interactions are partially compensated for by an adverse conformational entropy term as the peptide backbone becomes more constrained in DMSO. However, the increase of the entropy term ($-T\Delta S$) is overcompensated for by a larger decrease in the enthalpic contribution (ΔH) when changing the solvent from methanol to DMSO.

The hydrophobic contribution to β-hairpin stability

Comparison of the thermodynamic parameters of the diastereomeric compounds **7a** and **7b** in the same solvent provides an opportunity to estimate the impact of the hydrophobic interactions on hairpin stability. As described above, in methanol solution, the high contribution of the electrostatic interaction (*i.e.* hydrogen bonding) conceals the rather small hydrophobic stabilizing effect. In the less competitive, polar solvent DMSO, the extent of the hydrophobic effect can be estimated. The observed peptide melting curves indicate that the close neighborhood of apolar amino acid side chains provides significant stability. Thus, the van der Waals interaction has a higher influence on hairpin folding than the simultaneous, destabilizing steric crowding. In DMSO solution, a melting point for diastereomer **7a** more than 30 K higher than that of diastereomer **7b** indicates the extent of the influence of hydrophobic interactions on β-hairpin population.

Conclusions

The present investigation of the (*S,S*)- and (*R,S*)-diastereomers of a hairpin mimetic allowed the qualitative evaluation of the importance of intramolecular hydrogen bonding on β-hairpin stability in several solvents to be carried out.

The population difference of the mimetics observed in solvents possessing different polarity and ability to compete (chloroform < dimethylsulfoxide < methanol) indicates the critical role of hydrogen bonding in hairpin stability.

Comparison of the thermodynamic constants of the two diastereomeric compounds in the same solvent allowed a quantitative evaluation of the hydrophobic effect to be made. The observed significantly higher thermodynamic stability of **7a** compared to **7b** in DMSO solution suggests that the hydrophobic effect might have significant influence on hairpin stability in polar solvents. The similar behavior of the diastereomers in methanol solution indicates that in such a small model system, the effect of a competing solvent dominates over weak hydrophobic forces. For a complete understanding of the role of hydrophobic effects on hairpin stability, a study involving larger diastereomer model hairpins will be necessary. Investigations in this direction are in progress.

The experimental results could not be reproduced in every respect by computational studies. The calculations performed using the OPLS-AA force field predicted that the β-hairpin conformation of the (*R,S*)-diastereomer would be more probable than that of the (*S,S*)-diastereomer (21% compared to 16%),the opposite of what is observed experimentally. The failure of the calculations might be attributable to overestimation of the importance of steric repulsions.

Experimental

Materials

Starting materials were purchased from commercial suppliers and were used without further purification. Diethylamine, diisopropylethylamine, (trimethylsilyl)acetylene, $Pd(PPh_3)_2Cl_2$, *N*,*O*-bis(trimethylsilyl)acetamide and 2-iodoaniline were obtained from Aldrich. Methyl-2-iodobenzoate was from Lancaster, cuprous iodide from Merck, *O*-(7-azabenzotriazol-1-yl)-*N*,*N*,*N*′,*N*′-tetramethyluronium hexafluorophosphate and dimethylformamide were obtained from Fluka, hexane from J. T. Baker, and L-valine and L-alanine methyl ester were purchased from Bachem. Ethyl acetate was from Riedel-de Haën.

Microwave heating

The method used is described in ref. 41.

Sonochemistry

The sonochemical reactions were performed at ambient temperature using a VCX 500 ultrasonic processor (Sonics and Materials INC) equipped with a 13 mm diameter probe. 50% Amplitude was selected for the irradiations.

HPLC

The separation of compound **7a** and **7b** was performed on a Gilson HPLC system connected to a Dynamax 83-121 C column (60 Å) and a Dynamax absorbance detector (Model UV-1) working at 254 nm.

Theoretical conformational analysis

The conformational energy calculations were performed using the OPLS-AA all-atom force field as implemented in the program Macromodel 7.0.[42] The general born solvent accessible (GB/SA) surface area method developed by Still[43] was used in all calculations. The number of torsion angles allowed to vary during each Monte Carlo step ranged from 1 to $n-1$, where n is the total number of rotatable bonds. Amide bonds were fixed in the *trans* configuration. Conformational searches were conducted by use of the systematic unbound multiple minimum (SUMM) search method[44] implemented in the Batchmin program. First, 20 000 Monte Carlo step runs were performed (4000 steps on 5 processors with the command NPRC, at the Centre for Parallel Computers, KTH, Stockholm) and those conformations within 25 kJ mol^{-1} of the global minimum were kept. PR conjugate gradient minimization with a maximum of 1000 iterations was used in the conformational search. In the subsequent minimization to fully converged structures, a maximum of 50 000 steps of PRCG and/or truncated Newton conjugated gradient (TNCG) minimization was used.

Circular dichroism spectroscopy

CD spectra were measured on a JASCO J-810 spectropolarimeter from 190 to 360 nm using a 0.2 mm path length cell. 5 Scans were accumulated at ambient temperature with a scanning speed of 100 nm min^{-1}, using 50 μmol dm^{-3} methanol solutions. Optical rotation was measured with a Perkin-Elmer 241 polarimeter.

Infrared spectroscopy

IR spectra were obtained on a Perkin Elemer 1600 series FTIR instrument; recording 16 scans on 10 mol dm^{-3} samples in $CHCl_3$ solution using a 1 mm cuvette.

Mass spectrometry

Mass spectra (EI, 70 eV) were obtained with a Hewlett Packard 5971 Series mass selective detector interfaced with a Hewlett Packard 5890 Series II gas chromatograph equipped with a DB-1 (25 m × 0.20 mm) capillary column. The ESI-MS of compound **7a** and **7b** was obtained with a Finnigan ThermoQuest AQA mass spectrometer (ESI 30 eV, probe temperature 100 °C) equipped with a Gilson 322-H2 gradient pump system and a SB-C18 column. A water–acetonitrile–formic acid (0.05%) mobile phase was used with a gradient of 20 to 80% acetonitrile over 10 min.

NMR spectroscopy

NMR spectra were recorded on a Jeol JNM EX400 spectrometer (^{1}H at 399.8 MHz, ^{13}C at 100.5 MHz), a Varian UNITY spectrometer (^{1}H at 399.95 MHz, ^{13}C at 100.6 MHz), and on a JEOL JNM EX270 spectrometer (^{1}H at 270.2 MHz, ^{13}C at 67.8 MHz). Chemical shifts are referenced indirectly to TMS *via* the ^{2}H lock signal. Exchange of amide protons with deuterons was affected by dissolving the sample (*ca.* 10 mg) in a 1:1:1 mixture of D_2O–CD_3OD–acetone-d_6 (1 mL), followed by evaporation of the solvent after 3 h. NOE effects were measured from NOESY and ROESY spectra with mixing times between 0.7 and 1.5 s. In the 1D NOE difference experiments, a saturation time of 20 s was used.

Thermodynamic analysis

The NMR melting curve of each proton investigated was first analysed using reciprocal temperature plots and its first-order derivative. The thermodynamic parameters T_m and ΔH_m estimated in this way (eqn. 1 and 2) were used as initial conditions in the restricted least-squares calculations fitting of the experimental data to eqn. 3§§ using Scientist (Windows version 1.04, MicroMath Inc., Salt Lake City, UT, USA). Method details are described by Honda and co-workers.[40a,b]

$$\delta_{obs} = \delta_F + (\delta_U - \delta_F)f \quad (1)$$

$$\Delta H_m = \frac{4R}{\delta_F - \delta_U}\left[\frac{d\delta}{d\left(1/T\right)}\right]_m \quad (2)$$

$$\delta_{obs} = \delta_U + \frac{\delta_F - \delta_U}{1 + \exp\left[\frac{-\Delta H_m}{R}\left(\frac{1}{T} - \frac{1}{T_m}\right)\right]} \quad (3)$$

X-Ray crystallography

Details of the X-ray crystallographic analysis of the structure of **7a** are given in the ESI.

CCDC reference number 183993. See http://www.rsc.org/suppdata/nj/b1/b111241d/ for crystallographic data in CIF or other electronic format.

Synthesis

Scheme 1 outlines the methodology used to prepare the (*S*)-Val, (*S*)-Ala-derivative (**7a**) and the (*R*)-Val, (*S*)-Ala derivative (**7b**) of 2-amido-2′-carboxamidotolane. (*S*)-*N*-Acetylvaline was prepared by acetylation of (*S*)-valine under sonochemical conditions.[45] (*S*)-Alaninemethylamide was obtained by transamidation of (*S*)-alanine methyl ester following literature procedures.[46] Subjecting 2-iodoaniline (**1**) to Sonogashira coupling with (trimethylsilyl)acetylene afforded 2-[(trimethylsilyl)ethynyl]aniline (**2**) in excellent yield, [41] desilylation by potassium fluoride[47] yielded 2-ethynylaniline (**3**). Reaction of compound **3** with methyl-2-iodobenzoate under the conditions used in step c gave 2-amino-2′-carboxymethyldiphenylacetylene (**4**). *O*-(7-Azabenzotriazol-1-yl)-*N*,*N*,*N*′,*N*′-teramethyluronium hexafluorophosphate (HATU)-mediated coupling of **4** with (*S*)-*N*-acetylvaline yields **5**. The amino group of **4** is sterically and inductively deactivated, making this step unusually difficult. Therefore, the amino group was activated with *N*,*O*-bis(trimethylsilyl)acetamide (BSA) in dichloromethane for 30 min. The carboxyl group was allowed to react for 20 min with HATU in a mixture of diisopropylethylamine, dichloromethane, and dimethylformamide. The two solutions were then combined and stirred for 72 h, giving **5** in 52% isolated yield. Alternatively, the modified procedure of Roshchin and Bumagin.[48] gave 45% yield in 20 h. **5** was then hydrolysed and racemized using four equivalents of potassium *tert*-butoxide in diethyl ether, affording **6** in quantitative yield. The benzoic acid derivative **6** was then coupled to (*S*)-alaninemethylamide using HATU as the coupling reagent, resulting in a mixture of hairpin mimetic diastereomers **7a** and **7b**. The mixture was purified by column chromatography on silica using ethyl acetate as eluent, followed by separation of the two diastereomers by preparative HPLC (ethyl acetate eluent). This procedure allowed us to synthesize the two diastereomers in parallel in an efficient manner. Two methods for the selective synthesis of **7a** were earlier described by Kemp and Li,[16e] but no yields were reported.

(*S*)-2-Acetylamino-3-methylbutyric acid. (*S*)-Valine (470.6 mg, 4 mmol) was dissolved in water (10 mL) and was sonicated for 6 min.[45] Acetic acid anhydride (0.75 mL, 8 mmol) was added at 0, 2, and 4 min. Then, the mixture was concentrated on a rotatory evaporator. The residue was dissolved in methanol and the solution filtered, concentrated on a rotatory evaporator, and the remaining solvent removed under reduced pressure overnight, giving (*S*)-2-acetylamino-3-methylbutyric acid as a white solid in 99% yield (629.5 mg, 4.0 mmol). ^{1}H NMR (400 MHz, D_2O, 25 °C): δ 4.17 [d, ^3J(H,H) = 5.9 Hz, 1H, CH_α], 2.11 [dh, ^3J(H,H) = 4.8, 5.9 Hz, 1H, CH_β], 1.98 (s, 3H, $COCH_3$), 0.89 [2d, ^3J(H,H) = 4.8 Hz, 6H, $CH_{3\gamma}$]. ^{13}C NMR (100 MHz, D_2O, 25 °C) δ 175.7, 174.5, 58.6, 29.8, 21.6, 18.3, 17.2.

(*S*)-2-Amino-*N*-methyl-propionamide. (*S*)-Alanine methyl ester hydrochloride (1.00 g, 7.2 mmol) was treated with 40% methylamine in water (60 mL) following the literature procedure.[46] The solution was stirred at 40 °C for 80 min, and then concentrated under reduced pressure. The residue was dissolved in ethanol (253 K) and treated with diethyl ether (253 K) until a white precipitate was observed. The precipitate (methylamine salt) was filtered off and the filtrate was concentrated on a rotatory evaporator, followed by removal of the remaining solvent under reduced pressure, giving 2-amino-*N*-methylpropionamide as a white solid in 84% yield (611.0 mg, 6.0 mmol). ^{1}H NMR (400 MHz, D_2O, 25 °C): δ 3.58 [q, ^3J(H,H) = 6.9 Hz, 1H; CH_α], 2.71 (s, 3H; NH–CH_3), 1.27 [d, ^3J(H,H) = 6.9 Hz, 3H; CH_3]. ^{13}C NMR (100 MHz, D_2O, 25 °C) δ 176, 49.9, 25.9, 19.0.

2-[(Trimethylsilyl)ethynyl]aniline (2). 2-Iodoaniline (**1**) (394 mg, 1.8 mmol), $Pd(PPh_3)_2Cl_2$ (25.6 mg, 0.04 mmol), CuI (13.8 mg, 0.08 mmol), (trimethylsilyl)acetylene (0.28 mL, 2.00 mmol), diethylamine (3.0 mL, 27.20 mmol), and dimethylformamide (0.5 mL) were stirred under nitrogen in a heavy-

§§ The original reference[40b] contains an erroneous version of eqn. 3.

walled Smith process vial at 120 °C for 5 min under microwave irradiation. Then, the reaction mixture was poured into 0.1 M aqueous HCl (5–10 mL) and extracted three times with diethyl ether (5–10 mL). The combined organic layers were washed with conc. aqueous $NaHCO_3$ solution (5–10 mL) and water (5–10 mL), re-extracting the aqueous phases twice in each case with diethyl ether, then concentrated under reduced pressure. Thereafter, the residue was purified by flash chromatography (silica gel 60, particle size 0.040–0.063 mm, Merck; hexane–ethyl acetate 12:1). The combined product fractions were concentrated on a rotatory evaporator, followed by removal of the remaining solvent under reduced pressure overnight, yielding **2** as a brown oil in 98% yield (331.8 mg, 1.76 mmol).[41] ^{1}H NMR (400 MHz, $CDCl_3$, 25 °C): δ 7.29 [dd, J(H,H) = 1.7, 7.5 Hz, 1H; ArH], 7.11 [ddd, J(H,H) = 1.7, 7.5, 8.2 Hz, 1H; ArH], 6.68 [dd, J(H,H) = 1.1, 8.2 Hz, 1H; ArH], 6.66 [ddd, J(H,H) = 1.1, 7.5, 7.5 Hz, 1H; ArH], 4.07 (br s, 2H; NH_2), 0.27 [s, 9H; $RSi(CH_3)_3$]. ^{13}C NMR (100 MHz, $CDCl_3$, 25 °C) δ 148.2, 132.2, 129.8, 117.7, 114.1, 107.7, 101.7, 99.8, 0.0. MS (70 eV, EI): m/z (%) 189 (61) $[M]^+$, 174 (100). IR ($CHCl_3$): ν 3617.2, 3474.8, 3383.7, 3019.1, 2967.8, 2893.8, 2141.8, 1611.5, 1490.6, 1454.3 cm^{-1}.

2-Ethynylaniline (3). Following the literature procedure,[47] compound **2** (331.8 mg, 1.76 mmol) was dissolved in methanol (10 mL) and $KF{\cdot}2H_2O$ (495.0 mg, 5.3 mmol) was added. The mixture was stirred for 7 h at room temperature and thereafter concentrated under reduced pressure. The residue was dissolved in diethyl ether and water was added. The organic phase was separated, and the aqueous phase was re-extracted three times. The combined organic phases were concentrated under reduced pressure, giving compound **3** as a yellowish solid in 97% yield (198.8 mg, 1.7 mmol). ^{1}H NMR (400 MHz, $CDCl_3$, 25 °C): δ 7.32 [dd, J(H,H) = 1.6, 7.6 Hz, 1H; ArH], 7.15 [ddd, J(H,H) = 1.6, 7.4, 7.4 Hz, 1H; ArH], 6.70 [dd, J(H,H) = 0.9, 7.4 Hz, 1H; ArH], 6.68 [ddd, J(H,H) = 0.9, 7.4, 7.6 Hz, 1H; ArH], 4.25 (br s, 2H; NH_2). ^{13}C NMR (100 MHz, $CDCl_3$, 25 °C) δ 148.6, 132.7, 130.2, 117.9, 114.4, 106.7, 82.5, 80.7. MS (70 eV, EI): m/z (%) 117 (100) $[M]^+$, 90 (60). IR ($CHCl_3$) ν 3496.5, 3399.6, 3302.7, 2927.1, 2854.4, 2091.2, 1609.5, 1488.4, 1458.1 cm^{-1}.

2-(2′-Aminophenylethynyl)benzoic acid methyl ester (4). Compound **3** (200.2 mg, 1.71 mmol), 2-iodobenzoic acid methyl ester (493.0 mg, 1.88 mmol), $Pd(PPh_3)_2Cl_2$ (24.0 mg, 0.034 mmol), CuI (13.0 mg, 0.068 mmol), diethylamine (1.5 mL, 13.60 mmol), and dimethylformamide (0.5 mL) were stirred under nitrogen in a heavy-walled Smith process vial at 120 °C for 5 min under microwave irradiation. Then, the reaction mixture was filtered through Celite and was poured into 0.1 M aqueous HCl (5–10 mL). The mixture was extracted three times with diethyl ether (5–10 mL). The combined organic layers were washed with conc. aqueous $NaHCO_3$ solution (5–10 mL) and water (5–10 mL), re-extracting the aqueous phases twice in each case with diethyl ether, filtered through magnesium sulfate, and then concentrated under reduced pressure. Thereafter, the residue was purified by flash chromatography (silica gel 60, particle size 0.040–0.063 mm, Merck; hexane–ethyl acetate 9:1). The combined product fractions were concentrated on a rotatory evaporator, followed by removal of the remaining solvent under reduced pressure overnight, giving **4** as a white solid in 78% yield (336.3 mg 1.33 mmol). ^{1}H NMR (400 MHz, $CDCl_3$, 25 °C): δ 8.02 [ddd, J(H,H) = 0.6, 1.36, 8.0 Hz, 1H; ArH], 7.67 [ddd, J(H,H) = 0.6, 1.4, 7.8 Hz, 1H; ArH], 7.51 [ddd, J(H,H) = 1.36, 7.48, 7.80 Hz, 1H; ArH], 7.40 [ddd, J(H,H) = 1.40, 7.48, 7.90 Hz, 1H; ArH], 7.30 [ddd, J(H,H) = 0.56, 1.56, 7.67 Hz, 1H; ArH], 7.15 [ddd, J(H,H) = 1.56, 7.32, 8.11 Hz, 1H; ArH], 6.74 [ddd, J(H,H) = 0.56, 1.12, 8.11 Hz, 1H; ArH], 6.68 [ddd, J(H,H) = 1.12, 7.67, 7.32 Hz, 1H; ArH], 5.17 (br s, 2H; NH_2), 3.94 (s, 3H; CH_3). ^{13}C NMR (100 MHz, $CDCl_3$; 25 °C) δ 166.2, 149.6, 133.7, 132.0, 131.9, 130.5, 130.2, 130.2, 127.3, 124.7, 117.1, 114.1, 107.2, 93.6, 92.5, 52.3. MS (70 eV, EI): m/z (%) 251 (83) $[M]^+$, 219 (100), 190 (44). IR ($CHCl_3$) ν 3690.3, 3489.1, 3369.5, 3023.5, 2395.6, 2207.7, 1716.5, 1623.2, 1491.6 cm^{-1}.

(*S*)-2-[2′-(2″-Acetylamino-3″-methylbutyrylamino)phenylethynyl]benzoic acid methyl ester (5). Compound **4** (60.7 mg, 0.24 mmol) dissolved in dichloromethane (1 mL) was treated with BSA (0.06 mL, 0.24 mmol) for 30 min. 2-Acetylamino-3-methylbutyric acid was dissolved in a mixture of dichloromethane (2 mL), dimethylformamide (1 mL), and diisopropylethylamine (0.21 mL, 1.21 mmol). HATU (286.6 mg, 1.21 mmol) was added and the mixture was stirred for 20 min. The two solutions were combined and the mixture was stirred for 72 h. Thereafter, the reaction mixture was poured into 0.1 M aqueous HCl (5–10 mL) and extracted three times with diethyl ether (5–10 mL). The combined organic layers were washed with conc. aqueous $NaHCO_3$ solution (5–10 mL) and water (5–10 mL), re-extracting the aqueous phases twice in each case with diethyl ether, filtered through magnesium sulfate, and then concentrated under reduced pressure. The residue was purified by flash chromatography (silica gel 60, particle size 0.040–0.063 mm, Merck; hexane–ethyl acetate 1:1). The combined product fractions were concentrated on a rotatory evaporator, followed by removal of the remaining solvent under reduced pressure overnight, giving **5** as white solid in 52% yield (49.1 mg 0.13 mmol). Alternatively, the modified procedure of Roshchin and Bumagin.[48] gave 45% yield in 20 h. ^{1}H NMR (400 MHz, $CDCl_3$, 25 °C): δ 9.50 (br s, 1H; NH), 8.55 [dd, J(H,H) = 1.2, 8.2 Hz, 1H; ArH], 8.12 [ddd, J(H,H) = 0.6, 1.4, 8.3 Hz, 1H; ArH], 7.68 [ddd, J(H,H) = 0.6, 1.4, 7.8 Hz, 1H; ArH], 7.57 [ddd, J(H,H) = 1.40, 7.5, 7.8 Hz, 1H; ArH], 7.53 [ddd, J(H,H) = 1.6, 7.1, 8.3 Hz, 1H; ArH], 7.42 [dd, J(H,H) = 1.4, 7.4 Hz, 1H; ArH], 7.36 [ddd, J(H,H) = 1.1, 1.4, 8.3 Hz, 1H; ArH], 7.09 [ddd, J(H,H) = 1.4, 7.6, 7.6 Hz, 1H; ArH], 6.48 [d, ^3J(H,H) = 7.9 Hz, 1H; NH], 5.30 [dd, ^3J(H,H) = 5.9, 7.9 Hz, 1H; CH_α], 4.14 (s, 3H; CH_3), 2.20 [dh, ^3J(H,H) = 5.9, 6.8 Hz, 1H; CH_β], 2.04 (s, 3H; CH_3), 1.01 [d, ^3J(H,H) = 6.8 Hz, 3H; CH_3], 0.96 [d, ^3J(H,H) = 6.8 Hz, 3H; CH_3]. ^{13}C NMR (100 MHz, $CDCl_3$, 25 °C) δ 171.2, 169.7, 166.3, 140.1, 133.8, 132.4, 132.0, 130.8, 130.0, 129.9, 128.2, 124.0, 123.4, 119.7, 112.2, 95.7, 90.4, 57.7, 53.4, 32.8, 23.4, 19.2, 17.8. MS (70 eV, EI): m/z (%) 392 (6) $[M]^+$, 281 (9), 251 (100), 207 (58), 72 (76). IR ($CHCl_3$) ν 3422.5, 3322.2, 2400.0, 1716.0, 1666.0, 1578.5, 1525.4, 1509.8, 1447.3 cm^{-1}.

(*S*)-2-[2′-(2″-Acetylamino-3″-methylbutyrylamino)phenylethynyl]benzoic acid (6). Compound **5** (390.9 mg, 1.0 mmol) was dissolved in diethyl ether (5 mL) and dichloromethane (1 mL). A suspension of potassium *tert*-butoxide (446.7 mg, 4.0 mmol) in diethyl ether (20 mL) was added to this solution and the mixture was stirred for 15 h. Then, the suspension was extracted with chloroform. The combined organic layers were filtered through magnesium sulfate, then concentrated on a rotatory evaporator, followed by removal of the remaining solvent under reduced pressure, giving **5** as brown solid in 99% yield (373.0 mg, 0.98 mmol). ^{1}H NMR (270 MHz, $CDCl_3$, 25 °C): δ 9.57 (br s, 1H; NH), 8.47 [d, ^3J(H,H) = 8.6 Hz, 1H; ArH], 8.09 [d, ^3J(H,H) = 7.3 Hz, 1H; ArH], 7.66 [d, ^3J(H,H) = 7.6 Hz, 1H; ArH], 7.51–7.56 (m, 2H; ArH), 7.32–7.44 (m, 2H; ArH), 7.09 [t, ^3J = 7.6 Hz, 1H; ArH], 6.90 (bs, 1H; NH), 5.30 [dd, ^3J(H,H) = 4.3, 7.3 Hz, 1H; CH_α], 2.10 (s, 3H; CH_3), 1.22 [dh, ^3J(H,H) = 5.9, 7.6 Hz, 1H; CH_β], 0.99 [2d, ^3J(H,H) = 5.9 Hz, 6H; CH_3]. ^{13}C (67.9 MHz, $CDCl_3$, 25 °C) δ 170.9, 170.88, 168.4, 139.9, 133.1, 132.1, 132.0, 131.3, 130.6, 129.9, 128.2, 123.6, 119.7, 112.5, 95.2, 90.0, 58.5, 33.2,

31.1, 23.6, 19.2, 18.2. IR ($CHCl_3$) ν 3412.2, 3309.7, 2400.0, 1698.0, 1681.0, 1659.6, 1582.7, 1522.9, 1450.3 cm^{-1}.

2-[2′-(2″-Acetylamino-3″-methylbutyrylamino)phenylethynyl]-*N*-(1-methylcarbamoylethyl)benzamide (7). Compound **6** (373.0 mg, 1.0 mmol) was dissolved in dichloromethane (14 mL), diisopropylethylamine (1.57 mL, 0.12 mol) and HATU (943.3 mg, 4.0 mmol) was added, and the mixture was stirred for 1 h. 2-Amino-*N*-methylpropionamide (411.5 mg, 4.0 mmol) dissolved in a mixture of dimethylformamide (3 mL), dichloromethane (1 mL), and diisopropylethylamine (0.1 mL) was added and the solution was stirred for 140 min. Then, the reaction mixture was poured into 0.1 M aqueous HCl (5–10 mL). The mixture was extracted three times with diethyl ether (5–10 mL). The combined organic layers were washed with conc. aqueous $NaHCO_3$ solution (5–10 mL) and water (5–10 mL), re-extracting the aqueous phases twice in each case with diethyl ether, filtered through magnesium sulfate, and then concentrated under reduced pressure. Thereafter, the residue was purified by flash chromatography (silica gel 60, particle size 0.040–0.063 mm, Merck; ethyl acetate). The combined product fractions were concentrated on a rotatory evaporator. The diastereomeric mixture was separated by HPLC using ethyl acetate as eluent, giving 129.1 mg of compound **7a** and 107.1 mg of **7b**, 51% yield (236.2 mg, 0.1 mmol).

*(S,S)-2-[2′-(2″-Acetylamino-3″-methylbutyrylamino)phenylethynyl]-N-(1-methylcarbamoylethyl)benzamide (**7a**).* ^{1}H NMR (400 MHz, $CDCl_3$, 25 °C): δ 9.33 (br s, 1H; NH), 8.61 [d, ^3J(H,H) = 8.4 Hz, 1H; ArH], 7.91 [d, ^3J(H,H) = 4.7 Hz, 1H; NH], 7.63–7.68 (m, 2H; ArH), 7.46–7.53 (m, 2H; ArH), 7.33–7.40 (m, 2H; ArH), 7.14 [d, ^3J(H,H) = 8.1 Hz; NH], 7.06 [dd, ^3J(H,H) = 7.5, 7.5 Hz, 1H; ArH], 6.60 [d, ^3J(H,H) = 9.3 Hz, 1H; NH], 5.50 [dd, ^3J(H,H) = 5.2, 9.3 Hz, 1H; Val-CH_α], 5.32 [dq, ^3J(H,H) = 6.8, 8.4 Hz, 1H; Ala-CH_α], 2.76 [d, ^3J(H,H) = 4.7 Hz, 3H; CH_3^{NHAla}], 2.33 [dh, ^3J(H,H) = 5.2, 6.6 Hz, 1H; Val-CH_β], 2.1 (s, 3H, CH_3^{COVal}), 1.49 [d, ^3J(H,H) = 6.8 Hz, 3H; Ala-CH_3], 1.05 [d, ^3J(H,H) = 6.6 Hz, 3H; Val-$CH_{3\gamma}$], 0.95 [d, ^3J(H,H) = 6.6 Hz, 3H; Val-$CH_{3\gamma}$]. ^{13}C NMR (100 MHz, $CDCl_3$, 25 °C) δ 173.5,171.3, 170.6, 166.5, 140.3, 135.2, 133.9, 132.3, 130.9, 129.8, 128.3, 127.3, 123.4, 122.3, 119.4, 112.1, 94.9, 89.5, 57.7, 48.5, 32.8, 26.0, 23.7, 20.4, 19.2, 17.2. MS (30 eV, ESI): m/z (%) 463 (100) $[M-H]^+$. IR ($CHCl_3$) ν 3412.9, 3307.1, 2972.5, 2935.8, 2876.4, 1648.7, 1578.9, 1514.2 cm^{-1}.$[\alpha]_D^{20}$ = +64° (c = 1, $CHCl_3$).

*(R,S)-2-[2′-(2″-Acetylamino-3″-methylbutyrylamino)phenylethynyl]-N-(1-methylcarbamoylethyl)benzamide (**7b**).* ^{1}H NMR (400 MHz, $CDCl_3$, 25 °C): δ 9.68 (br s, 1H; NH), 8.63 [d, ^3J(H,H) = 8.4 Hz, 1H; ArH], 7.89 [d, ^3J(H,H) = 4.7 Hz, 1H; NH], 7.71 [d, ^3J(H,H) = 7.7 Hz, 1H; ArH], 7.65 [d, ^3J(H,H) = 7.5 Hz, 1H; ArH], 7.45–7.52 (m, 2H; ArH), 7.30–7.42 (m, 2H; ArH), 7.06 [t,^3J(H,H) = 7.5 Hz, 1H; ArH], 6.96 [d, ^3J(H,H) = 9.0 Hz; NH], 6.68 [d, ^3J(H,H) = 9.1 Hz, 1H; NH], 5.65 [dd, ^3J(H,H) = 4.4, 9.1 Hz, 1H; Val-CH_α], 5.26 [dq,^3J(H,H) = 7.0, 9.0 Hz, 1H; Ala-CH_α], 2.81 [d, ^3J(H,H) = 4.7 Hz, 3H; CH_3^{NHAla}], 2.25 [dh,^3J = 4.4, 6.8 Hz, 1H; Val-CH_β], 2.1 (s, 3H; CH_3^{COVal}), 1.36 [d, ^3J(H,H) = 7.0 Hz, 3H; Ala-CH_3], 0.94 [d, ^3J(H,H) = 6.8 Hz, 3H; Val-$CH_{3\gamma}$], 0.87 [d, ^3J(H,H) = 6.8 Hz, 3H; Val-$CH_{3\gamma}$]. ^{13}C NMR (100 MHz, $CDCl_3$, 25 °C) δ 173.6, 171.4, 170.3, 166.3, 140.8, 135.6, 133.3, 132.0, 130.8, 129.8, 128.3, 127.0, 123.3, 122.3, 119.3, 112.0, 94.6, 89.6, 57.3, 48.5, 33.2, 26.0, 23.7, 19.9, 19.3, 17.0. MS (30 eV, ESI): m/z (%) 463 (46) $[M-H]^+$, 432 (24), 322 (100), 291 (9), 263 (7). IR ($CHCl_3$) ν 3413.3, 3307.6, 2973.3, 2933.5, 2875.2, 1653.0, 1580.0, 1517.7 cm^{-1}. $[\alpha]_D^{20}$ = −64° (c = 1, $CHCl_3$).

Acknowledgements

The Centre for Parallel Computers (PDC) at the Royal Institute of Technology (KTH), Stockholm, Sweden, is acknowledged for a generous allotment of computing time. We thank G. Lindeberg, A. Johansson, and E. Åkerblom for helpful discussions.

References

1 N. C. J. Strynadka, S. E. Jensen, P. M. Alzari and M. N. G. James, *Nat. Struct. Biol.*, 1996, **3**, 290.
2 (*a*) J. D. Puglishi, L. Chen, S. Blanchard and A. D. Frankel, *Science*, 1995, **270**, 1200; (*b*) G. Variani *Acc. Chem. Res.*, 1997, **30**, 189.
3 (*a*) P. E. Floreancing, S. E. Swalley, J. W. Trauger and P. B. Dervan, *J. Am. Chem. Soc.*, 2000, **122**, 6342; (*b*) R. E. Bremer, J. W. Szewczyk, E. E. Baird and P. B. Dervan, *Bioorg. Med. Chem.*, 2000, **8**, 1947–1955.
4 (*a*) J. Collinge *Annu. Rev. Neurosci.*, 2001, **24**, 519; (*b*) M. Mihara, Y. Takahashi and A. Ueno, *Biopolymers*, 1998, **47**, 83; (*c*) K. M. Pan, M. Baldwin, J. Nguyen, M. Gasset, A. Serban, D. Groth, I. Mehlhorn, Z. Huang, R. J. Fletterick, F. E. Cohen and S. B. Prusiner, *Proc. Natl. Acad. Sci. U. S. A.*, 1993, **90**, 10 962; (*d*) R. Riek, S. Hornemann, G. Wider, M. Billeter, R. Glockshuber and K. Wuthrich, *Nature*, 1996, **382**, 180.
5 (*a*) L. C. Serpell, C. C. F. Blake and P. E. Fraser, *Biochemistry*, 2000, **39**, 13 269; (*b*) S. Ohnisiki, A. Koide and S. Koide, *J. Mol. Biol.*, 2000, **301**, 477; (*c*) D. R. Booth, M. Sunde, V. Bellotti, C. V. Robinson, W. L. Hutchinson, P. E. Fraser, P. N. Hawkins, C. M. Dodson, S. E. Radford, C. C. F. Blake and B. M. Pepys, *Nature*, 1997, **385**, 787.
6 J. M. McDonnell, D. Fushman, S. M. Cahill, B. J. Sutton and D. Cowburn, *J. Am. Chem. Soc.*, 1997, **119**, 5321.
7 (*a*) J. P. Derrick, G. J. Davies, Z. Dauter, K. S. Wilson and D. B. Wigley, *J. Mol. Biol.*, 1992, **227**, 1253; (*b*) J. P. Derrick and D. B. Wigley, *Nature*, 1992, **359**, 752; (*c*) J. P. Derrick and D. B. Wigley, *J. Mol. Biol.*, 1994, **243**, 906; (*d*) C. Boutillon, R. Wintjens, G. Lippens, H. Drobecq and A. Tartar, *Eur. J. Biochem.*, 1995, **231**, 166; (*e*) E. L. McCallister, E. Alm and D. Baker, *Nat. Struct. Biol.*, 2000, **7**, 669.
8 (*a*) P. D. Kwong, R. Wyatt, J. Robinson, R. W. Sweet, J. Sodroski and W. A. Hendrickson, *Nature*, 1998, **393**, 648; (*b*) A. Cochran, R. T. Tong, M. A. Starovanski, E. J. Park, R. S. McDowell, J. E. Theaker and N. J. Skelton, *J. Am. Chem. Soc.*, 2001, **123**, 625.
9 (*a*) B. Odaert, F. Jean, C. Boutillon, E. Buisine, O. Melnyk, A. Tartar and G. Lippens, *Protein Sci.*, 1999, **8**, 2773; (*b*) C. Das, S. Raghothama and P. Balaram, *J. Am. Chem. Soc.*, 1998, **120**, 5812; (*c*) E. Alba, A. Jiménez and M. Rico, *J. Am. Chem. Soc.*, 1997, **119**, 175.
10 (*a*) H. J. Dyson and P. E. Wright, *Annu. Rev. Biophys. Chem.*, 1991, **20**, 519; (*b*) V. Munoz and L. Serrano, *Proteins*, 1994, **20**, 301; (*c*) T. P. Quinn, N. B. Tweedy, R. W. Williams, J. S. Richardson and D. C. Richardson, *Proc. Natl. Acad. Sci. U. S. A.*, 1994, **91**, 8747.
11 (*a*) B. L. Sibanda and J. M. Thornton, *J. Mol. Biol.*, 1993, **229**, 428; (*b*) B. L. Sibanda and J. M. Thornton, *Nature*, 1985, **316**, 170
12 For reviews on β-hairpin mimetics, see: (*a*) M. S. Searle *J. Chem. Soc., Perkin Trans. 2*, 2001, 1011; (*b*) J. A. Robinson *Synlett*, 1999, **4**, 429; (*c*) J. S. Nowick, E. M. Smith and M. Pairish, *Chem. Soc. Rev.*, 1996, 401.
13 (*a*) D. L. Minor, Jr. and S. P. Kim, *Nature*, 1994, **367**, 660; (*b*) C. K. Smith, J. M. Withka and L. Regan, *Biochemistry*, 1994, **33**, 5510; (*c*) P. Y. Chou and G. D. Fasman, *Biochemistry*, 1973, **13**, 211; (*d*) K. Smith and L. Regan, *Acc. Chem. Res.*, 1997, **30**, 153; (*e*) K. Gunasekaran, C. Ramakrishnan and P. Balaram, *Protein Eng.*, 1997, **10**, 1131.
14 S. J. Russel and A. G. Cochran, *J. Am. Chem. Soc.*, 2000, **123**, 625.
15 (*a*) I. Pozdnyakova, J. Guidry and P. Wittung-Stafshede, *J. Am. Chem. Soc.*, 2000, **122**, 6337; (*b*) A. C. Gibbs, L. H. Kondejewski, W. Gronwald, A. M. Nip, R. S. Hodges, B. D. Sykes and D. S. Wishart, *Nat. Struct. Biol.*, 1998, **5**, 284; (*c*) D. Tolkatchev, A. Ng, W. Vranken and F. Ni, *Biochemistry*, 2000, **39**, 2878.
16 (*a*) M. J. Soth and J. S. Nowick, *J. Org. Chem.*, 1999, **64**, 276; (*b*) S. C. Shankaramma, S. K. Singh, A. Sathyamurthy and P. Balaram, *J. Am. Chem. Soc.*, 1999, **121**, 5360; (*c*) T. S. Haque, J. C. Little and S. H. Gellman, *J. Am. Chem. Soc.*, 1996, **118**,

6975; (*d*) Y. J. Chung, B. R. Huck, L. A. Christianson, H. E. Stanger, S. Krauthäuser, D. R. Powell and S. H. Gellman, *J. Am. Chem. Soc.*, 2000, **122**, 3995; (*e*) D. S. Kemp and Z. Q. Li, *Tetrahedron Lett.*, 1995, **36**, 4175; (*f*) D. S. Kemp and Z. Q. Li, *Tetrahedron Lett.*, 1995, **36**, 4179; (*g*) J. S. Nowick and F. Insaf, *J. Am. Chem. Soc.*, 1997, **119**, 10 903; (*h*) J. S. Nowick *Acc. Chem. Res.*, 1999, **32**, 287; (*i*) P. Chitnumsub, W. R. Fiori, H. A. Lashuel, H. Diaz and J. W. Kelly, *Bioorg. Med. Chem.*, 1999, **7**, 39.

17 (*a*) I. L. Karle, S. K. Awasthi and P. Balaram, *Proc. Natl. Acad. Sci. U. S. A.*, 1996, **93**, 8189; (*b*) B. L. Sibanda, T. L. Blundell and J. M. Thornton, *J. Mol. Biol.*, 1989, **206**, 759.

18 T. S. Haque, J. C. Little and S. H. Gellman, *J. Am. Chem. Soc.*, 1994, **116**, 4105–4106.

19 (*a*) D. L. Minor, Jr. and P. S. Kim, *Nature*, 1994, **371**, 264; (*b*) F. Xu and A. Cross, *Magn. Reson. Chem.*, 1998, **36**, 651.

20 A. G. Street and S. L. Mayo, *Proc. Natl. Acad. Sci. U. S. A.*, 1999, **96**, 9074.

21 (*a*) K. L. Constantine, L. Mueller, N. H. Andersen, H. Tong, C. F. Wandler, M. S. Friedrichs and R. E. Bruccoleri, *J. Am. Chem. Soc.*, 1995, **117**, 10 841; (*b*) M. S. Friadrichs, T. R. Stouch, R. E. Bruccoleri, L. Mueller and K. L. Constantine, *J. Am. Chem. Soc.*, 1995, **117**, 10 855.

22 (*a*) G. P. Dado and S. H. Gellman, *J. Am. Chem. Soc.*, 1993, **115**, 4228; (*b*) E. Gallo and S. H. Gellman, *J. Am. Chem. Soc.*, 1993, **115**, 9774; (*c*) E. Gallo and S. H. Gellman, *J. Am. Chem. Soc.*, 1994, **116**, 11 560.

23 (*a*) K. Y. Tsang, H. Diaz, N. Graciani and J. W. Kelly, *J. Am. Chem. Soc.*, 1994, **116**, 3988; (*b*) H. Wang and S. S. Sung, *J. Am. Chem. Soc.*, 2000, **122**, 1999; (*c*) A. J. Maynard, G. J. Sharman and M. S. Searle, *J. Am. Chem. Soc.*, 1998, **120**, 1996.

24 T. S. Haque and S. H. Gellman, *J. Am. Chem. Soc.*, 1997, **119**, 2303.

25 M. S. Searle, S. R. Griffith-Jones and H. Skinner-Smith, *J. Am. Chem. Soc.*, 1999, **121**, 11 615.

26 G. J. Sharman and M. S. Searle, *J. Am. Chem. Soc.*, 1998, **120**, 5291.

27 (*a*) L. Belvisi, C. Gennari, A. Mielgo, D. Potenza and C. Scolastico, *Eur. J. Org. Chem.*, 1999, 389; (*b*) R. R. Gardner, G. B. Liang and S. H. Gellman, *J. Am. Chem. Soc.*, 1999, **121**, 1806.

28 L. Halab and W. D. Lubell, *J. Org. Chem.*, 1999, **64**, 3312.

29 D. Ranganathan, V. Haridas, S. Kurur, R. Nagaraj, E. Bikshapathy, A. C. Kunwar, A. V. S. Sarma and M. Vairamani, *J. Org. Chem.*, 2000, **65**, 365.

30 F. X. Schmid, in *Protein Structure: A Practical Approach*, ed. T. E. Creighton, IRL Press, Oxford, 1997, ch. 11, pp. 261–297.

31 (*a*) H. Tsunematsu, R. Isobe, K. Mizusaki, S. Makisumi and M. Yamamoto, *Org. Mass Spectrom.*, 1994, **29**, 260; (*b*) H. Tsunematsu,R.,Isobe, H. Hanazono, Y. Soeda, M. Inagaki, N. Ito, R. Higuchi and M. Yamamoto, *Chem. Pharm. Bull.*, 1999, **47**, 1040.

32 (*a*) H. Tsunematsu, S. Hachiyama,R.,Isobe, E. Ishida, M. Kakoi and M. Yamamoto, *Biochem. Biophys. Res. Commun.*, 1987, **146**, 907; (*b*) H. Tsunematsu, S. Nakashima and M. Yamamoto, *Org. Mass Spectrom.*, 1989, **24**, 943.

33 (*a*) A. Wokaun and R. R. Ernst, *Chem. Phys. Lett.*, 1977, **52**, 407; (*b*) A. J. Shaka and R. Freeman, *J. Magn. Reson.*, 1983, **51**, 169.

34 M. Perpick-Dumont, W. F. Reynolds and R. G. Enriquez, *Magn. Reson. Chem.*, 1988, **26**, 358.

35 (*a*) H. Kessler, C. Griesinger, J. Zarbock and H. R. Loosli, *J. Magn. Reson.*, 1984, **57**, 331; (*b*) H. Kessler, C. Griesinger and J. Lautz, *Angew. Chem., Int. Ed. Engl.*, 1984, **23**, 444; *Angew. Chem.*, 1984, **96**, 434; (*c*) H. Kessler, C. Griesinger and K. Wagner, *J. Am. Chem. Soc.*, 1987, **109**, 6927.

36 (*a*) A. Kumar, R. R. Ernst and K. Wuthrich, *Biochem. Biophys. Res. Commun.*, 1980, **95**, 1; (*b*) G. Bodenhausen, H. Kogler and R. R. Ernst, *J. Magn. Reson.*, 1984, **58**, 370.

37 A. Bax and D. G. Davis, *J. Magn. Reson.*, 1985, **63**, 207.

38 T. Parella *Magn. Reson. Chem.*, 1998, **36**, 467.

39 J. K. M. Sanders and J. D. Mersh, in *Progress in Nuclear Magnetic Resonance Spectroscopy*, ed. J. W. Emsley, J. Feeney and L. H. Sutcliffe, Pergamon Press, Oxford, 1982, vol. 15, pp. 353.

40 (*a*) S. Honda, N. Kobayashi and E. Munekata, *J. Mol. Biol.*, 2000, **295**, 269; (*b*) N. Kobayashi,S.,Honda, H. Yoshii and E. Munekata, *Biochemistry*, 2000, **39**, 6564; (*c*) S. Honda, N. Kobayashi, E. Munekata and H. Uedaira, *Biochemistry*, 1999, **38**, 1203.

41 M. Erdélyi and A. Gogoll, *J. Org. Chem.*, 2001, **66**, 4165.

42 F. Mohamadi, N. G. J. Richards, W. C. Guida, R. Liskamp, M. Lipton, C. Caufield, G. Chang, T. Hendrickson and W. C. Still, *J. Comput. Chem.*, 1990, **11**, 440.

43 W. C. Still, A. Tempczyk, R. C. Hawley and T. Hendrickson, *J. Am. Chem. Soc.*, 1990, **112**, 6127.

44 J. M. Goodman and W. C. Still, *J. Comput. Chem.*, 1991, **12**, 1110.

45 M. Pavlik, I. Kluh, F. Pavlikova, S. Vasickova and V. Kostka, *Collect. Czech. Chem. Commun.*, 1989, 1940.

46 R. W. Feenestra, E. H. M. Stokkingreef, A. M. Reichwein, W. B. H. Lousberg and H. C. J. Ottenheijm, *Tetrahedron*, 1990, **46**, 1745.

47 A. Arcadi, S. Cacchi and F. Marinelli, *Tetrahedron Lett.*, 1989, **30**, 2581.

48 A. I. Roshchin and N. A. Bumagin, *Chem. Heterocycl. Compd.*, 1999, **35**, 171.